NRL Report 6796

The Detection of Nonfluctuating Targets in Log-Normal Clutter

S. F. George

Radar Analysis
Radar Div.

October 4, 1968

CONTENTS

ABSTRACT

Measurements of sea clutter using high-resolution radar indicate that the cluter-cross-section returns follow a log-normal probability density function more closely than the usually assumed Rayleigh law. This report develops the theory for the detection of a steady signal in log-normal clutter by first using a single pulse and then by using the sum of N pulses integrated noncoherently. Plots of the probability density of the envelope of the signal plus clutter show the function to be bimodal, an unexpected result. Curves are presented for the threshold bias, normalized to the median clutter voltage, versus the probability of false alarm for several values of the standard deviation σ and for various values of N. Probability of detection curves are presented for σ = 3, 6, and 9 dB, for N = 1, 3, 10, and 30 pulses, and for false alarm probabilities from 10^{-2} to 10^{-8}. The ratio of signal to median clutter required for detection increases markedly as σ increases because of the highly skewed clutter density.

Manuscript submitted August 21, 1968.

THE DETECTION OF NONFLUCTUATING TARGETS IN LOG-NORMAL CLUTTER

SUMMARY

Sea clutter measurements made by NRL using a high-resolution radar show that the clutter cross section tends to be log-normally distributed. A study of the log-normal clutter model, therefore, seemed appropriate, and this report presents the results of such a study.

First, a derivation is presented of the log-normal density function required to establish a family of threshold values for false alarm probabilities varying from 10^{-2} to 10^{-8} and for selected values of standard deviation σ. Plots of the clutter density show highly skewed tails as σ increases, resulting in greatly increased bias values as compared to the Rayleigh model.

Next, the distribution of the envelope of signal plus clutter for a single pulse is derived. Plots of probability densities show a bimodal function, which is an unexpected result. The bimodal shape holds for all values of signal-to-noise ratio (S/N) and for all values of σ, but the dual peaks draw closer together and the dip becomes less pronounced as σ increases. Formulas for the probability of detection are given, but these could not be evaluated in closed form, so they were programmed for the NRL CDC 3800 computer.

Then the probabilities of false alarm and detection are developed for the sum of N pulses integrated noncoherently. The general method used is that of the characteristic function, which essentially requires two applications of the Fourier integral. Here again no solution in closed form seemed readily obtainable, so the CDC 3800 was programmed for numerical evaluation, using the fast Fourier transform technique.

Sets of curves are presented for the probability of detection for values of σ = 3, 6, and 9 dB, for N = 1, 3, 10, and 30 pulses, and for false alarm probabilities from 10^{-2} to 10^{-8}. The S/N required for detection for σ = 3 dB are about the same as those for the Rayleigh model, as would be expected since the log-normal tail for this case compares to the Rayleigh tail. However, as σ increases, the required S/N also rises markedly as a result of the increasingly skewed distributions. It should be noted that the S/N defined in this report uses the median clutter value for noise and not the usual rms value.

INTRODUCTION

Clutter-cross-section measurements of sea return taken with high-resolution radar show more of a tendency to follow a log-normal probability distribution than the Rayleigh distribution usually assumed. Data reported by NRL (1) using an X-band radar with a 0.02-μsec pulse are plotted in Fig. 1 on probability paper with the clutter cross section σ_c in dB on an arbitrary scale. A log-normal distribution is indicated by these points falling in a straight line. It is seen that the cumulative probability closely fits a line between 5% and 80%. Accurate data at the extremes are difficult to obtain, because thermal noise limits the low σ_c values and the system dynamic range limits the high σ_c values.

Studies made by Miner (2) and Ballard (3) also consider the log-normal description of the sea-clutter cross section and relate the standard deviation of the distribution to the

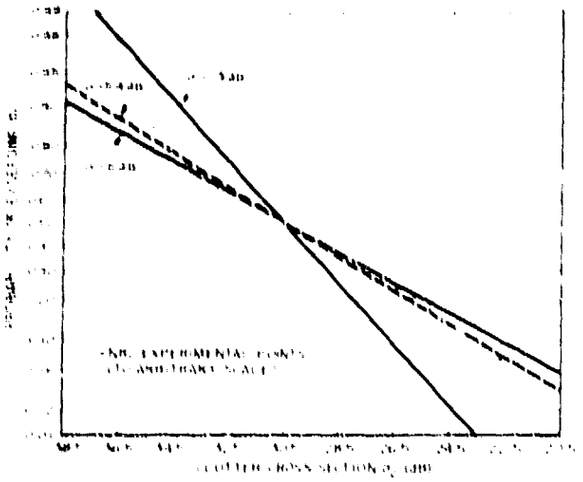

Fig. 1 - Probability distribution for the log-normal clutter model, with experimental points for an X-band radar with a 0.03-μsec pulse

radar illuminated patch area. Ballard actually set up a log-normal probability model but did not calculate detection curves. The present report follows much of the same theoretical method and extends the model to include the integration of N pulses.

LOG-NORMAL CLUTTER MODEL

If we assume that clutter cross section is log-normally distributed, then the probability density is given by

$$p(\sigma_c) = \frac{1}{\sqrt{2\pi}\,\sigma\,\sigma_c} \exp\left[-\frac{1}{2\sigma^2}\left(\ln\frac{\sigma_c}{\sigma_m}\right)^2\right], \tag{1}$$

where σ_c is the clutter cross section, σ_m is the median value of σ_c, and σ is the standard deviation of $\ln\sigma_c$ (natural logarithm). Since cross-section values are measures of power, the standard deviation (s.d.) is expressed in "natural units" (4) by the relationship

$$\sigma(\text{natural units}) = (0.1 \ln 10)\,\sigma(\text{dB}) = 0.2303\,\sigma(\text{dB}). \tag{2}$$

The value of σ in Fig. 1 is in dB, and σ must be converted into natural units by Eq. (2) for use in Eq. (1).

In Fig. 1 the log-normal probability distribution function is plotted for σ = 3 dB and σ = 6 dB. The dashed line is a close fit to the NRL experimental results on sea clutter previously mentioned. For this line, σ = 5.4 dB. From Ref. 3, a value of σ = 4.7 dB resulted from a clutter patch size of 3840 sq yd in a sea state 4. From the NRL studies (1), σ = 5.4 dB corresponds roughly to a clutter patch size of 135 sq yd in sea state 1.*

To determine the probability of false alarm and subsequently the probability density function of a signal plus clutter, Eq. (1) must first be transformed into a voltage-amplitude

*In general σ increases directly with sea state and inversely with clutter patch size.

density. If we let v_c be the envelope of the radar echo from the clutter area a_c, then $v_c = a_c^{1/2}$ or $a_c = kv_c^2$. Using this substitution in Eq. (1) yields

$$p(v_c) = \sqrt{\frac{2}{\pi}} \frac{1}{\sigma v_c} \exp\left[-\frac{1}{2\sigma^2}\left(2 \ln \frac{v_c}{v_m}\right)^2\right], \quad 0 < v_c < \infty \tag{3}$$

where v_m is the median value of v_c and σ remains the s.d. of $\ln a_c$. Then, σ is still measured according to Eq. (2).

The probability of false alarm for a voltage bias level β is given by

$$P_{FA} = \int_{\beta}^{\infty} p(v_c)\, dv_c = \frac{1}{\sqrt{\pi}} \int_{\frac{\sqrt{2}}{\sigma} \ln \beta}^{\infty} \exp(-t^2)\, dt, \tag{4}$$

where $\beta = \beta / v_m$ is the normalized bias level. The integral in Eq. (4) is related to the error function, which is well tabulated.

DETECTION OF A NONFLUCTUATING SIGNAL IN CLUTTER

Let us assume a radar pulse return from a target which is a steady signal of constant amplitude v_s. The clutter return will be assumed to have the log-normal amplitude density function as given in Eq. (3) and a phase ϕ_c that is uniformly random over $-\pi < \phi_c < \pi$. The analysis can be performed as though the radar were operating as a cw system. If the signal and clutter voltages add linearly prior to envelope detection, then we can assume that the signal plus clutter may be represented by the two components

$$X = v_s + v_c \cos \phi_c \tag{5a}$$

and

$$Y = v_c \sin \phi_c, \tag{5b}$$

where X and Y are the in-phase and quadrature components of the signal plus clutter.

We can define two new variables X' and Y' such that their joint probability is that of the clutter alone:

$$X' = X - v_s = v_c \cos \phi_c \tag{6a}$$

and

$$Y' = Y = v_c \sin \phi_c. \tag{6b}$$

Then, the relationship between these joint distributions is

$$p(v_c, \phi_c)\, dv_c d\phi_c = \begin{vmatrix} \frac{\partial X'}{\partial v_c} & \frac{\partial X'}{\partial \phi_c} \\ \frac{\partial Y'}{\partial v_c} & \frac{\partial Y'}{\partial \phi_c} \end{vmatrix} p(X', Y')\, dX'dY' = v_c\, p(X', Y')\, dX'dY'. \tag{7}$$

But since v_c and ϕ_c are independent variables, $p(v_c,\phi_c)dv_c d\phi_c = p(v_c)dv_c p(\phi_c)d\phi_c = p(v_c)dv_c(1/2\pi)d\phi_c$. Hence, from Eqs. (3) and (7) we have

$$p(X',Y')\,dX'dY' = \frac{1}{\pi\sqrt{2\pi}\,\sigma v_c^2}\exp\left[-\frac{1}{2\sigma^2}\left(2\ln\frac{v_c}{v_m}\right)^2\right]dv_c d\phi_c. \tag{8}$$

From Eqs. (6) this becomes

$$p(X,Y) = \frac{1}{\pi\sqrt{2\pi}\,\sigma\,[(X-v_s)^2+Y^2]}\exp\left[-\frac{1}{2\sigma^2}\left(2\ln\frac{\sqrt{(X-v_s)^2+Y^2}}{v_m}\right)^2\right]. \tag{9}$$

Finally, using Eqs. (5) in Eq. (9) yields

$$p(v,\phi) = \frac{v}{\pi\sqrt{2\pi}\,\sigma\,(v^2-2v\,v_s\cos\phi+v_s^2)}\exp\left[-\frac{1}{2\sigma^2}\left(2\ln\frac{\sqrt{v^2-2vv_s\cos\phi+v_s^2}}{v_m}\right)^2\right] \tag{10}$$

where $v^2 = X^2 + Y^2$, $X = v\cos\phi$, $Y = v\sin\phi$, and the transformation from Eq. (9) to Eq. (10) is analogous to the one used in Eq. (7) with ϕ uniformly random from $-\pi$ to $+\pi$. Now v represents the envelope amplitude of signal plus clutter. The probability density function of v alone is obtained from Eq. (10) by

$$p(v) = 2\int_0^{\pi} p(v,\phi)\,d\phi. \tag{11}$$

Attempts to evaluate Eq. (11) in closed form were not successful, so computer numerical evaluation was employed. However, before illustrating the results, it is more meaningful to transform Eq. (10) into an expression containing a "psuedo" S/N, actually a signal-to-clutter ratio, since v_s is not easily obtained. If we let $r = v_s/v_m$ in Eq. (10) the probability density becomes

$$p(x,\phi) = \frac{x}{\pi\sqrt{2\pi}\,\sigma\,(x^2-2xr\cos\phi+r^2)}\exp\left[\frac{-2}{\sigma^2}\left(\ln\sqrt{x^2-2xr\cos\phi+r^2}\right)^2\right], \tag{12}$$

where $x = v/v_m$ is now the normalized envelope amplitude of signal plus clutter. Then the probability density function of x is

$$p(x) = 2\int_0^{\pi} p(x,\phi)\,d\phi. \tag{13}$$

The probability of detection for a single pulse of a steady signal in log-normal clutter for a normalized bias level γ is thus

$$P_D = \int_{\gamma}^{\infty} p(x)\,dx = 2\int_{\gamma}^{\infty}\int_0^{\pi} p(x,\phi)\,d\phi dx = 1 - 2\int_0^{\gamma}\int_0^{\pi} p(x,\phi)\,d\phi dx. \tag{14}$$

In Fig. 2 plots of Eq. (3) for various values of σ are compared with the Rayleigh distribution for which the median value has been set equal to v_m. It should be noted that the tail of the Rayleigh distribution falls off about as rapidly as that of the log-normal for σ = 3 dB, but the tail falls off less rapidly as σ becomes larger in the log-normal distribution. For these larger σ values, then, the bias values for a fixed P_{FA} are expected to be greater for the log-normal than for the Rayleigh distribution. Plots of bias values, obtained from Eq. (4), illustrate in Fig. 3 how rapidly the bias does increase as σ increases.

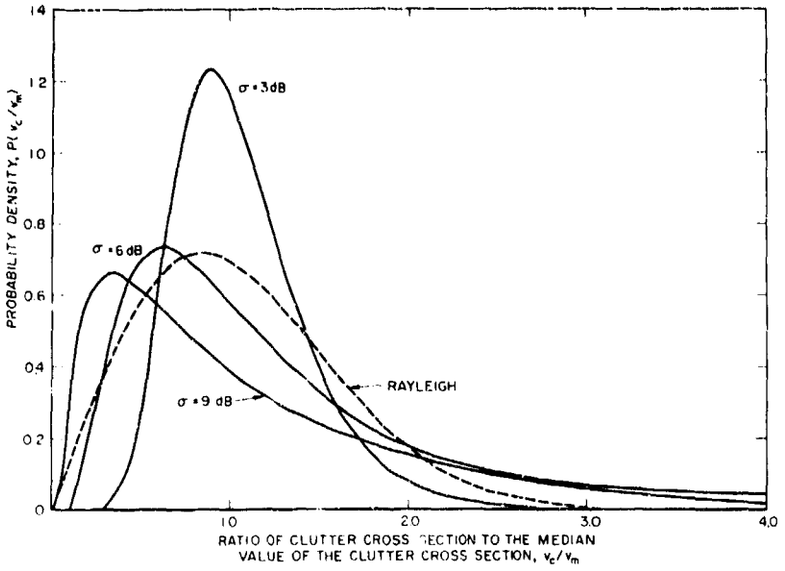

Fig. 2 - Log-normal probability density for σ = 3, 6, and 9 dB and the Rayleigh density for the median value v_m

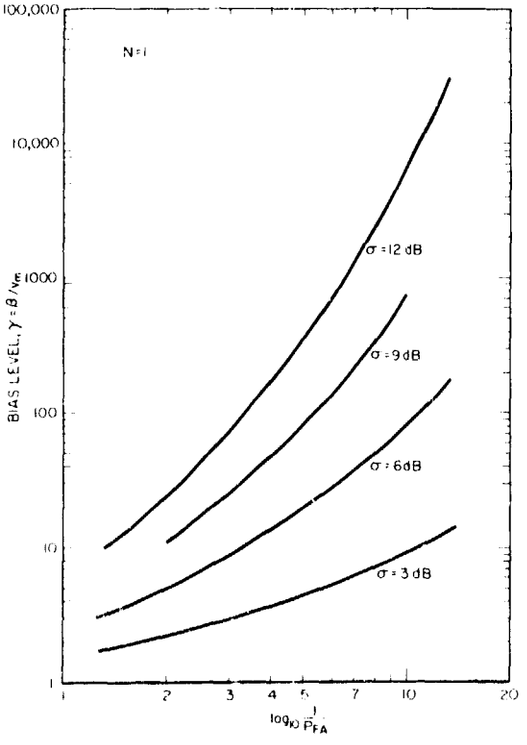

Fig. 3 - Bias levels as a function of false alarm probability with σ = 3, 6, 9, and 12 dB for N = 1, a single pulse of log-normal clutter

To plot the probability density function in Eq. (13) the integral had to be evaluated numerically, since no closed form solution was found. The CDC 3800 was programmed using Simpson's rule for the integration. Figure 4 shows a family of curves for the probability density of the envelope of signal plus clutter for σ = 3 dB and for several values of $r = v_s / v_m$ = S/N which has been designated as a voltage S/N. The double hump or bimodal curve is most unusual and surely not predicted. Note that this curve is the envelope distribution and hence assumes linear detection. The values of S/N shown are voltage ratios. Figure 5 shows curves for σ = 6 dB. Again the double hump is present but less pronounced. In Fig. 6 by increasing σ for a fixed value of r (i.e., S/N) the distributions remain bimodal but the humps tend to converge and the dip becomes less pronounced. Figures 4 and 5 show that as r increases, the curve shapes do not change substantially.

A word of caution is in order regarding the definition of the signal-to-noise ratio r = S/N = v_s / v_m. It should be noted that this is not the usual definition of the signal-to-noise ratio, where the noise is taken to be the rms value. Herein the noise (which is clutter) is taken to be the median value. This is a convenient definition to use and, also, one which would have considerable engineering significance, since clutter is frequently expressed in terms of its median value. However, in subsequent parts of this study where N pulses are integrated, care must be exercised in interpreting r. Since the log-normal model yields a two-parameter distribution, its behavior is more difficult to analyze and interpret than the Rayleigh model.

DETECTION USING THE SUM OF N PULSES

The straightforward method of determining the probability density for the sum of N envelope detected pulses, assuming they are independent, is by use of the characteristic

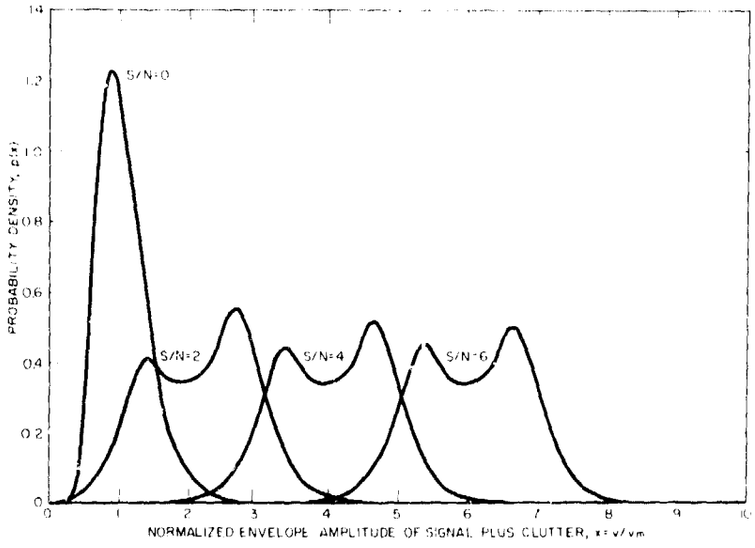

Fig. 4 - Probability densities of a single-pulse signal plus log-normal clutter for σ = 3 dB and voltage S/N = 0, 2, 4, and 6. Note the double peaks.

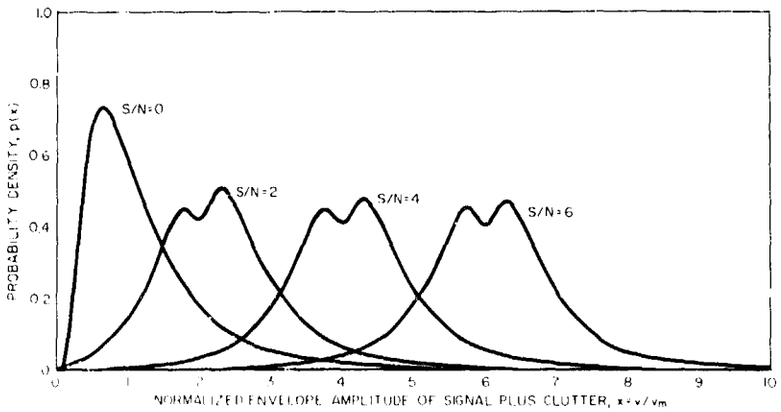

Fig. 5 - Probability densities of a single-pulse signal plus log-normal clutter for σ = 6 dB and voltage S/N = 0, 2, 4, and 6

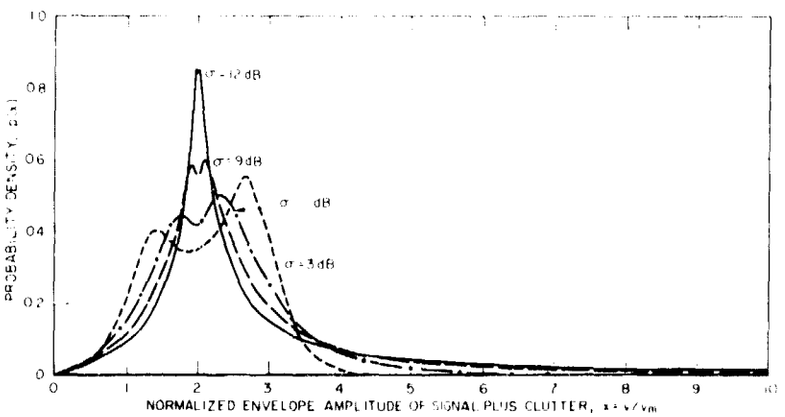

Fig. 6 - Probability densities of a single-pulse signal plus log-normal clutter for voltage S/N = 2 and σ = 3, 6, 9, and 12 dB.

function. Starting with the probability density of the envelope of signal plus clutter given by Eq. (13), the characteristic function is given by

$$\phi(w) = \int_0^\infty p(x) \exp(iwx)\, dx, \tag{15}$$

which is the Fourier transform (FT) of $p(x)$, since $x \geq 0$. The characteristic function for the sum of N independent pulses is

$$\phi_N(w) = [\phi(w)]^N. \tag{16}$$

It is noted that in general $\phi(w)$ is a complex function. Using the inverse FT of Eq. (16) gives the probability density for the sum of N pulses:

$$p_N(x) = \frac{1}{2\pi} \int_{-\infty}^{\infty} \phi_N(w) \exp(-iwx)\, dw. \tag{17}$$

Plots of Eq. (17) for $N = 1$, 2, and 3 and for S/N = 2 are shown in Fig. 7. Note that the double hump disappears as N increases. Also the distribution spreads out as N increases and begins to look more like a normal distribution.

For the sum of N pulses, the probability of false alarm is

$$p_N(FA) = \int_\gamma^\infty p_N(x)\, dx = 1 - \int_0^\gamma p_N(x)\, dx, \tag{18}$$

where $\gamma = 0$; and the probability of detection is

$$p_N(\text{Det.}) = 1 - \int_0^\gamma p_N(x)\, dx, \tag{19}$$

where $p_N(x)$ is evaluated for the parameter $\gamma \neq 0$. All attempts to find a closed-form expression for the integral in Eqs. (18) and (19) proved fruitless. Fortunately, the new digital technique known as the fast Fourier transform (FFT) made it possible to evaluate these integrals numerically in a reasonable time.

PROBABILITY OF DETECTION RESULTS

Bias values for $N = 3$, 10, and 30 were determined from Eq. (18) by numerical integration for false alarm probabilities from 10^{-2} to 10^{-8} and for $\sigma = 3$, 6, and 9 dB. These are plotted in Figs. 8 through 10. Curves for bias values are repeated in Figs. 11 through 13 with N varied for a fixed σ value.

Using these bias values, Eq. (19) is evaluated, giving the probability of detection versus S/N per pulse, in values of P_D from 0.1 to 0.9999. Figures 14 through 17 are for $\sigma = 3$ dB. A summary of P_D for $P_{FA} = 10^{-6}$ and $N = 1$, 3, 10, and 30 is presented in Fig. 18. In Figs. 19 through 23 detection curves are given for $\sigma = 6$ dB, and in Figs. 24 through 28 for $\sigma = 9$ dB. An inspection of these curves shows that the S/N required for detection increases rapidly as σ increases. In fact the S/N in dB appears to increase linearly as σ increases, doubling as σ goes from 3 to 6 dB and increasing by a factor of 3 as σ goes from 3 to 9 dB.

It is interesting to compare the set of curves for $\sigma = 3$ dB and $N = 1$ (no integration) with those obtained using a Gaussian model. Skolnik (5) shows that the S/N required compares favorably with the results using a log-normal model (Fig. 14) as should be expected for the $\sigma = 3$ dB case.

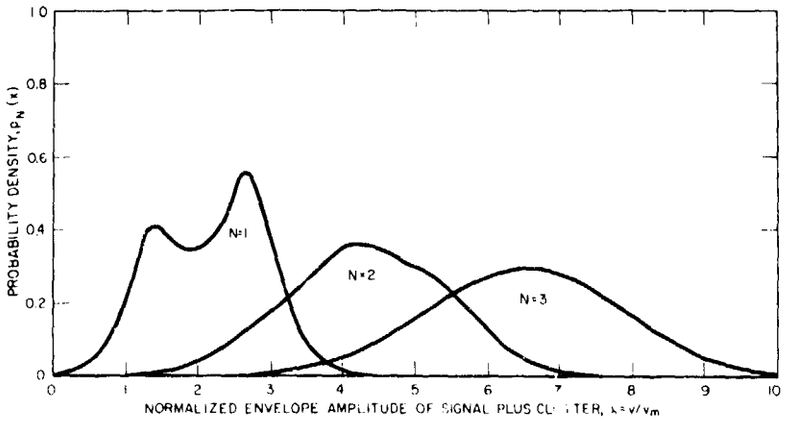

Fig. 7 - Probability densities of a signal plus log-normal clutter for σ = 3 dB, voltage S/N = 2, and number of pulses N = 1, 2, and 3. Note as N increases the curve looks more like a normal distribution.

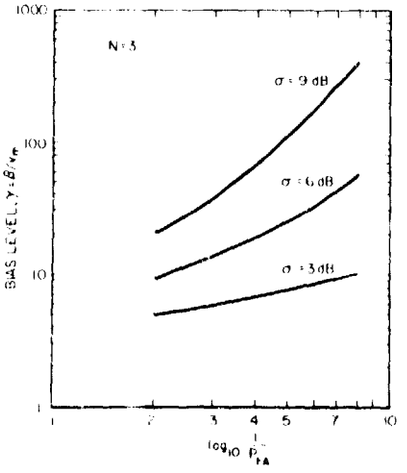

Fig. 8 - Bias levels for false alarm probabilities from 10^{-2} to 10^{-8} for N = 3 with σ = 3, 6, and 9 dB

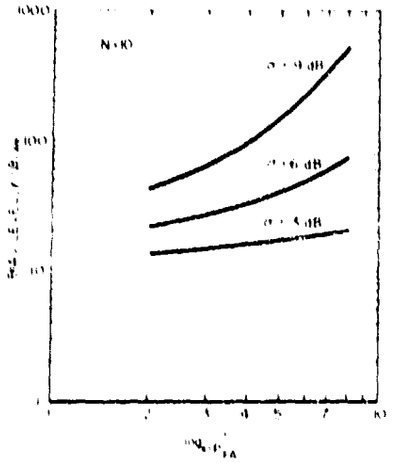

Fig. 9 - Bias levels for false alarm probabilities from 10^{-2} to 10^{-8} for $N = 10$ with $\sigma = 3$, 6, and 9 dB

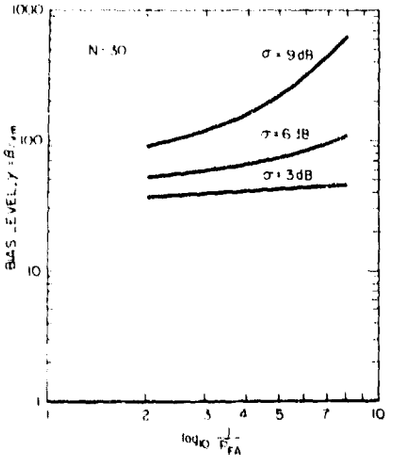

Fig. 10 - Bias levels for false alarm probabilities from 10^{-2} to 10^{-8} for $N = 30$ with $\sigma = 3$, 6, and 9 dB

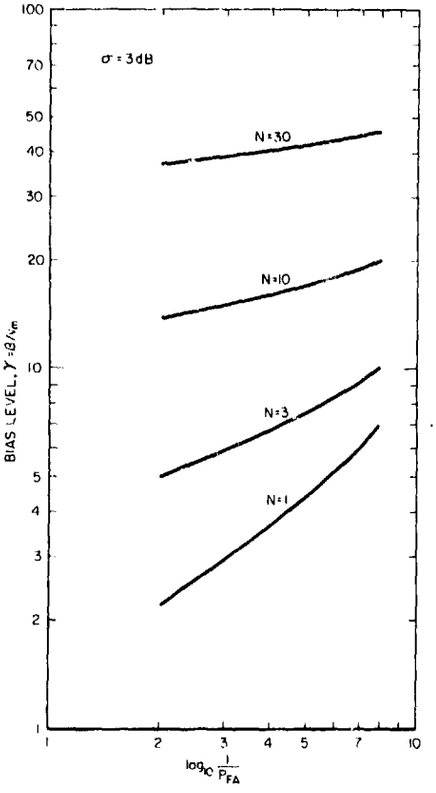

Fig. 11 - Bias levels for false alarm probabilities with the number of pulses integraded, N = 1, 3, 10, and 30 for σ = 3 dB

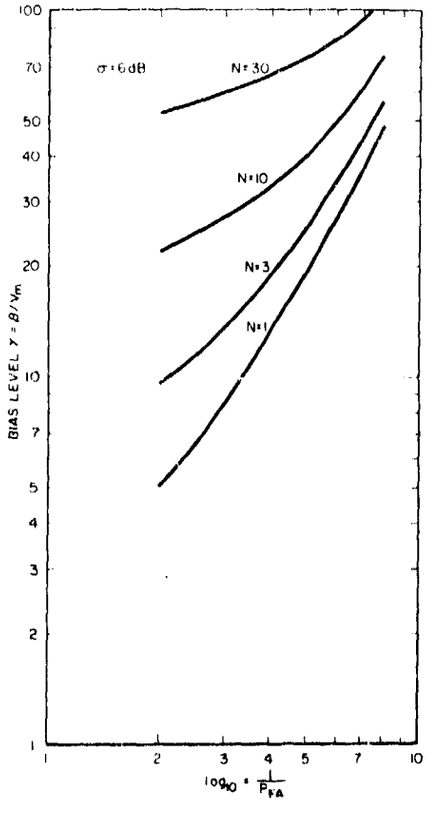

Fig. 12 - Bias levels for false alarm probabilities with the number of pulses integrated, N = 1, 3, 10, and 30 for σ = 6 dB

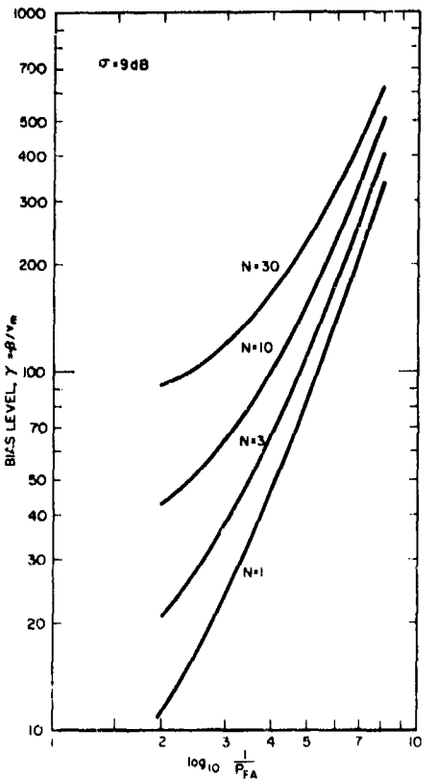

Fig. 13 - Bias levels for false alarm probabilities with the number of pulses integrated, N = 1, 3, 10, and 30 for σ = 9 dB

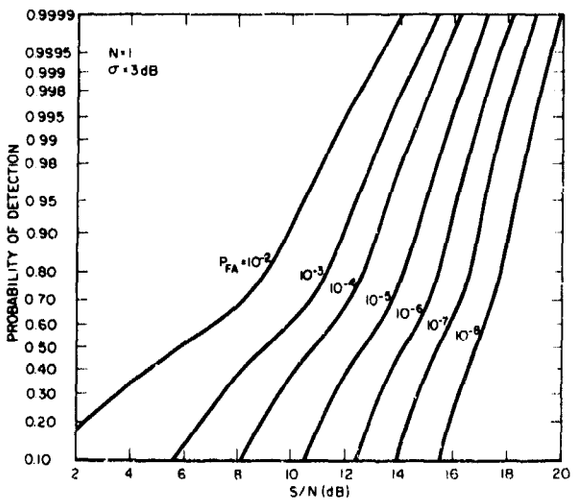

Fig. 14 - Probability of detection vs S/N for P_{FA} = 10^{-2} to 10^{-8} with σ = 3 dB and N = 1

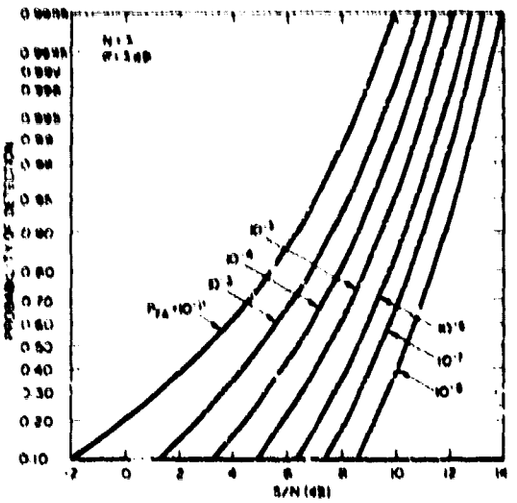

Fig. 15 - Probability of detection vs S/N for $P_{FA} = 10^{-2}$ to 10^{-8} with $\sigma = 3$ dB and $N = 3$

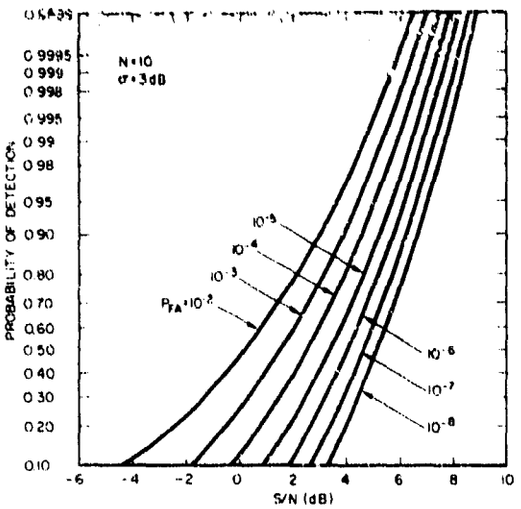

Fig. 16 - Probability of detection vs S/N for $P_{FA} = 10^{-2}$ to 10^{-8} with $\sigma = 3$ dB and $N = 10$

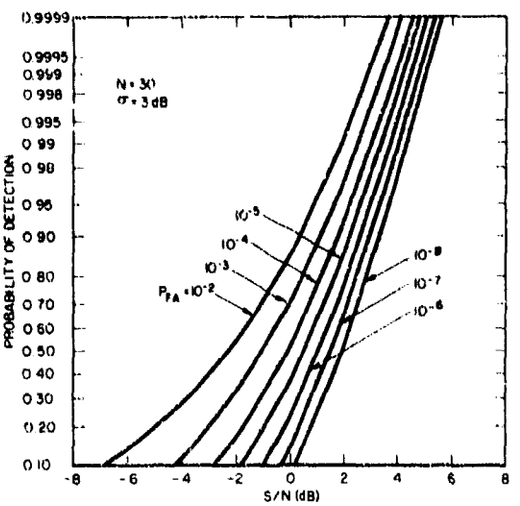

Fig. 17 - Probability of detection vs S/N for $P_{FA} = 10^{-2}$ to 10^{-8} with $\sigma = 3$ dB and $N = 30$

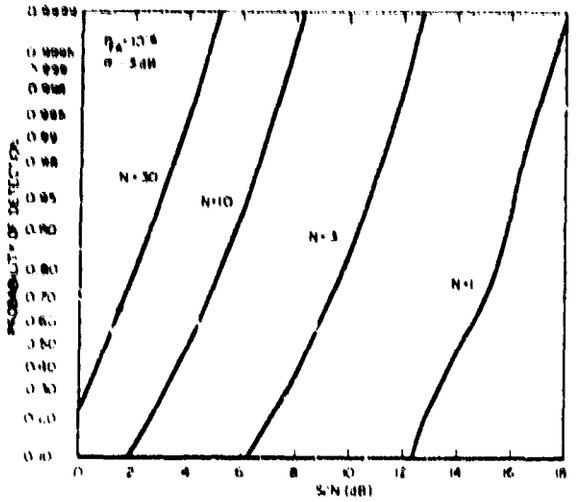

Fig. 18 - Probability of detection vs S/N for N = 1, 3, 10, and 30 with σ = 3 dB and $P_{FA} = 10^{-6}$

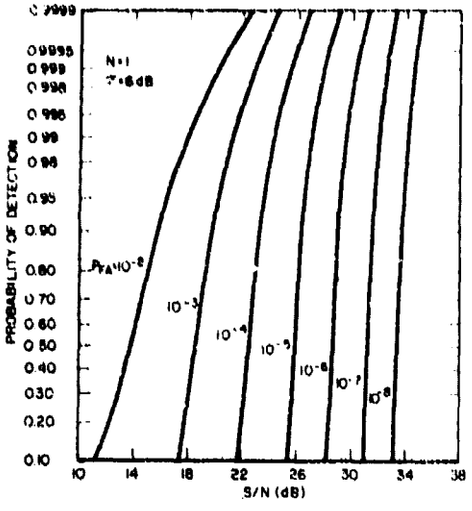

Fig. 19 - Probability of detection vs S/N for $P_{FA} = 10^{-2}$ to 10^{-8} with σ = 6 dB and N = 1

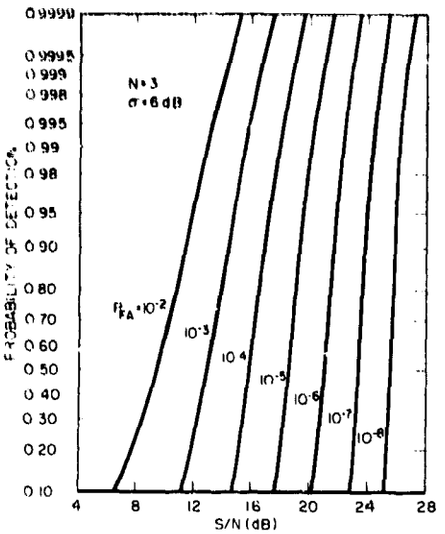

Fig. 20 - Probability of detection vs S/N for $P_{FA} = 10^{-2}$ to 10^{-8} with $\sigma = 6$ dB and $N = 3$

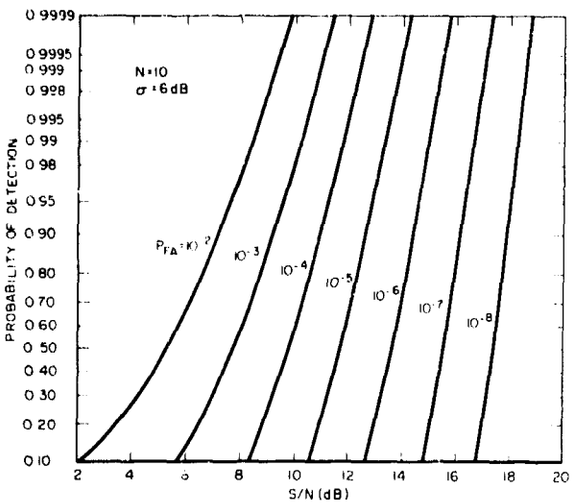

Fig. 21 - Probability of detection vs S/N for $P_{FA} = 10^{-2}$ to 10^{-8} with $\sigma = 6$ dB and $N = 10$

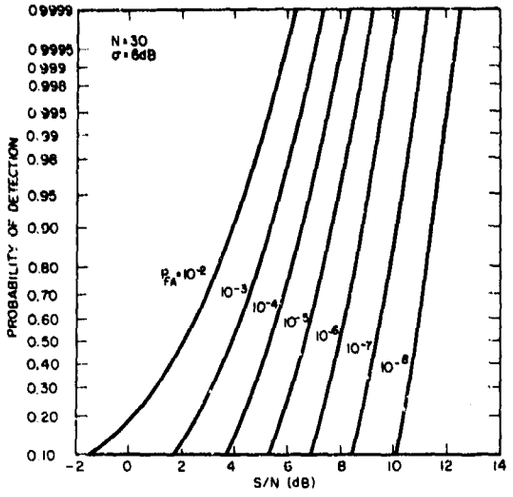

Fig. 22 - Probability of detection vs S/N for $P_{FA} = 10^{-2}$ to 10^{-8} with $\sigma = 6$ dB and $N = 30$

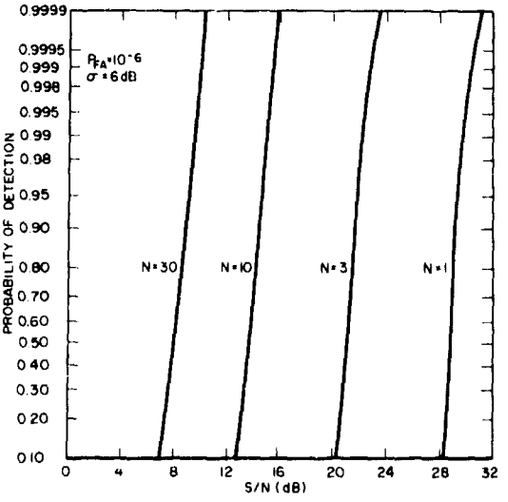

Fig. 23 - Probability of detection vs S/N for $N = 1$, 3, 10, and 30 with $\sigma = 6$ dB and $P_{FA} = 10^{-6}$

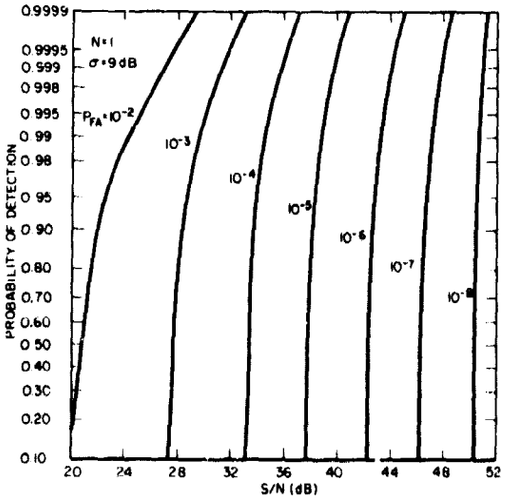

Fig. 24 - Probability of detection vs S/N for $P_{FA} = 10^{-2}$ to 10^{-8} with $\sigma = 9$ dB and $N = 1$

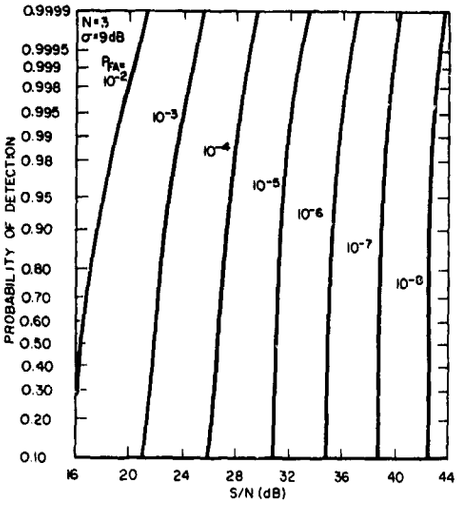

Fig. 25 - Probability of detection vs S/N for P_{FA} = 10^{-2} to 10^{-8} with σ = 9 dB and N = 3

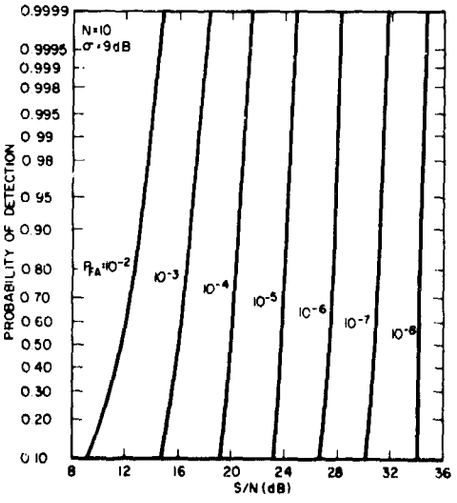

Fig. 26 - Probability of detection vs S/N for P_{FA} = 10^{-2} to 10^{-8} with σ = 9 dB and N = 10

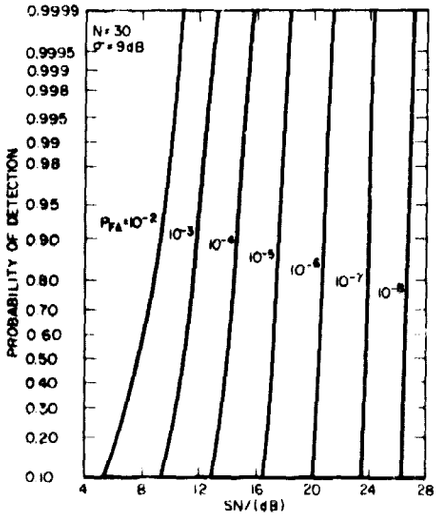

Fig. 27 - Probability of detection vs S/N for P_{FA} = 10^{-2} to 10^{-8} with σ = 9 dB and N = 30

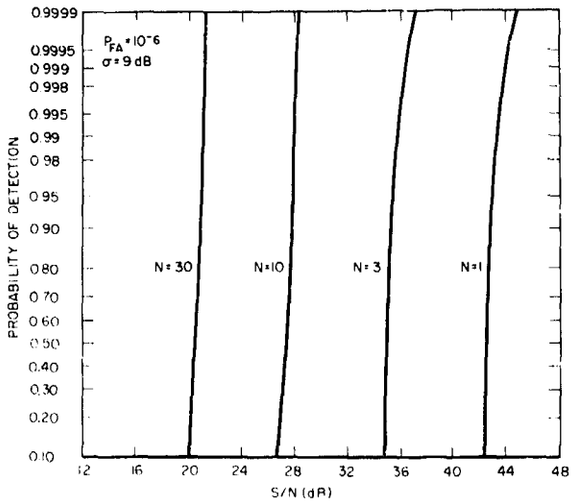

Fig. 28 - Probability of detection vs S/N for N = 1, 3, 10, and 30 with σ = 9 dB and P_{FA} = 10^{-6}

ACKNOWLEDGMENT

The author expresses his appreciation to G. V. Trunk of the Radar Analysis Staff for his many valuable discussions during the course of this work and Jon David Wilson of the Radar Analysis Staff for his helpfulness in the programming.

REFERENCES

1. Findlay, A.M., "Sea-Clutter Measurement by Radar-Return Sampling," NRL Report 6661, Feb. 12, 1968

2. Miner, R.Y., "Review of ASW Radar Sea Clutter," TRW Systems Doc. 7234:1:001 (Confidential Report, Unclassified Title), Feb. 8, 1966

3. Ballard, A.H., "Detection of Radar Signals in Log-Normal Sea-Clutter," TRW Systems Doc. 7425-8509-T0-000, May 31, 1966

4. Fenton, L.F., "The Sum of Log-Normal Probability Distributions in Scatter Transmission Systems," IRE Trans. on Comm. Systems CS-8, 57-67, Mar. 1960

5. Skolnik, M.I., "Introduction to Radar Systems," New York:McGraw-Hill, 1962

Security Classification

DOCUMENT CONTROL DATA - R & D

(Security classification of title, body of abstract and indexing annotation must be entered when the overall report is classified)

1. ORIGINATING ACTIVITY (Corporate author)	2a. REPORT SECURITY CLASSIFICATION
Naval Research Laboratory Washington, D.C. 20390	Unclassified
	2b. GROUP

3. REPORT TITLE

THE DETECTION OF NONFLUCTUATING TARGETS IN LOG-NORMAL CLUTTER

4. DESCRIPTIVE NOTES (Type of report and inclusive dates)

A final report on one phase of the problem

5. AUTHOR(S) (First name, middle initial, last name)

Samuel F. George

6. REPORT DATE	7a. TOTAL NO. OF PAGES	7b. NO. OF REFS
October 4, 1968	22	5

8a. CONTRACT OR GRANT NO.	9a. ORIGINATOR'S REPORT NUMBER(S)
b. PROJECT NO.	NRL Report 6796
c.	9b. OTHER REPORT NO(S) (Any other numbers that may be assigned this report)
d.	

10. DISTRIBUTION STATEMENT

This document has been approved for public release and sale; its distribution is unlimited.

11. SUPPLEMENTARY NOTES	12. SPONSORING MILITARY ACTIVITY
	Department of the Navy Naval Research Laboratory Washington, D.C. 20390

13. ABSTRACT

Measurements of sea clutter using high-resolution radar indicate that the clutter-cross-section returns follow a log-normal probability density function more closely than the usually assumed Rayleigh law. This report develops the theory for the detection of a steady signal in log-normal clutter by first using a single pulse and then by using the sum of N pulses integrated noncoherently. Plots of the probability density of the envelope of the signal plus clutter show the function to be bimodal, an unexpected result. Curves are presented for the threshold bias, normalized to the median clutter voltage, versus the probability of false alarm for several values of the standard deviation σ and for various values of N. Probability of detection curves are presented for σ = 3, 6, and 9 dB, for N = 1, 3, 10, and 30 pulses, and for false alarm probabilities from 10^{-2} to 10^{-8}. The ratio of signal to median clutter required for detection increases markedly as σ increases because of the highly skewed clutter density.

DD FORM 1 NOV 1473 (PAGE 1)

S/N 0101-807-6801

Security Classification

14 KEY WORDS	LINK A		LINK B		LINK C	
	ROLE	WT	ROLE	WT	ROLE	WT
High-resolution radar						
Sea clutter						
Signal detection						
Log-normal distributions						
Mathematical analysis						
Probability distributions						
Radar targets						